On-State Distortion in High Electron Mobility Transistor Microwave and RF Switch Control Circuits

Robert H. Caverly, *Senior Member, IEEE,* and Kennith J. Heissler

***Abstract*—The origin of the distortion generating mechanism in microwave and RF control circuits using high electron-mobility transistors (HEMT's) is presented in this paper. A model is presented for predicting the distortion in series-connected HEMT switches. The theoretical discussion shows that turn-off voltages in the range of 1.0–1.5 V provide the lowest distortion in series switch configurations. A comparison of the HEMT switch with MESFET switches shows that the HEMT switch generates more distortion than its MESFET counterpart. In addition, the frequency response of HEMT switches is the opposite of the MESFET switch, with less distortion at low frequencies. The model is validated with experimental data taken on a AlGaAs/GaAs HEMT in the series switch configuration.**

***Index Terms*—Microwave devices, microwave switches, nonlinearities.**

NOMENCLATURE

α_n	Current–voltage expansion coefficients.
ε_i	Dielectric permittivity of AlGaX layer (farad/meter).
μ_{LF}	Low-field two-dimensional electron gas (2DEG) mobility (meters^2/volt second).
μ_n	Mobility expansion coefficients (meters^2/volt^n -second).
γ	$v_{\rm gs} - v_{\rm ds}$ relationship.
Δd	2DEG layer thickness (meters).
C_D, C_G	Drain, source capacitance (farad).
$C_{\rm DG}$, $C_{\rm GS}$	Drain–gate, gate–source capacitance (farad).
d_i	AlGaX layer thickness (meters).
E	2DEG electric field (volts/meter).
$I_{\rm DS}$	High electron-mobility transistor (HEMT) drain–source current (amperes).
$I_{\rm DSat}$	HEMT $I_{\rm DS}$ saturation current (amperes).
$IP2$, $IP3$	Second- and third-order distortion intercept point (dBm).
L	HEMT gate length (meters).
$n_{\rm 2DEG}$	2DEG electron carrier density (coulomb/m^2).
q	Electronic charge (coulomb).
R_G, R_{GG}	Gate, leakage resistance (ohms).
R_C	Drain–source series resistance (ohms).
$v_{\rm SAT}$	Saturation velocity (meters/second).
$V_{\rm DS}$, $v_{\rm gs}$	HEMT dc, ac drain–source voltage (volts).
$V_{\rm GS0}$, $v_{\rm gs}$	HEMT dc, ac gate–source voltage (volts).
$V_{\rm Off}$	HEMT turn-off voltage (volts).
W	HEMT gatewidth (meters).
Z_0	Characteristic impedance of system (ohms).

Manuscript received January 22, 1999. This work was supported in part by the Office of Naval Research under Contact N000149810895, and by the National Science Foundation under Grant CCR-9805718.

R. H. Caverly is with the Department of Electrical and Computer Engineering, Villanova University, Villanova, PA 19085 USA (e-mail: r.caverly@ieee.org).

K. J. Heissler is with Lockheed Martin Government Electronics Systems, Moorestown, NJ 08057 USA.

Publisher Item Identifier S 0018-9480(00)00221-0.

I. INTRODUCTION

THE use of high electron-mobility transistors (HEMT's) is increasing in many microwave circuits and systems because of their high-frequency and high-speed response. These applications span the range from photonic and satellite communication systems to high-performance analog and digital integrated circuits [1]–[11]. In microwave applications such as integrated transceiver systems, HEMT's are often used in transmit and receive sections where each subsection shares a single antenna [4]–[6], [9]. In these systems, HEMT's can be used in series or series-shunt configurations as the signal control element connecting the transmitter and receiver subsystems to the antenna. In these microwave control applications, a dc voltage is applied to the gates of the devices to effect the switching action and allow microwave energy to flow with relatively low insertion loss through the 2DEG channel region. A complimentary gate voltage switches the device in the off state, creating high isolation between the switch ports.

There are many linear specifications that must be considered in designing an HEMT microwave control element, such as insertion loss, isolation, and power handling. A number of papers have been published describing the operation of HEMT's in these and other such applications [4]–[6], [9]. To date, however, there has not been a treatment of the device parameters that control the nonlinear distortion in microwave HEMT's control circuits. This nonlinear behavior of the HEMT while operating in a control mode will cause the introduction of unwanted signals into the circuit, creating harmonic or intermodulation products that can adversely affect system performance. The understanding of the underlying physical mechanism in HEMT's is important in creating a model of this phenomenon so that distortion may be predicted and controlled.

This paper presents the theoretical background describing the mechanism governing the nonlinearity in HEMT's switches. The general theoretical treatment allows the results to be used with a variety of HEMT technologies such as AlGaAs/GaAs and

AlGaN/GaN. From the theoretical discussion, a method to predict the distortion products as a function of HEMT electrical parameters are presented. The current–voltage characteristics of the HEMT operating in the linear region are derived using a simple charge density and field-dependent mobility model. From these characteristics, load referenced distortion intercept points are computed for both AlGaAs/GaAs and AlGaN/GaN HEMT control devices. The model is then verified against experimental data from a HEMT-based series switch.

II. Theoretical Discussion

A. Background

The nonlinear drain–source current–voltage characteristic of the HEMT will govern its production of unwanted distortion products. A general $I_{\rm DS}$–$V_{\rm DS}$ relationship for the HEMT that includes its nonlinear characteristics can be written as

$$I_{\rm DS} = \sum_{n=1}^{\infty} \alpha_n V_{\rm DS}^n \tag{1}$$

where the α_n contain terms dependent on the HEMT's electronic and microwave circuit parameters such as the gate bias circuitry, gate–drain, and gate–source leakage, and the device drain–source resistance R_C. A frequently used measure of distortion, the distortion intercept point, is derived for the microwave control element based on this $I_{\rm DS}$–$V_{\rm DS}$ characteristic. In general applications, the second- and third-order distortion intercept points ($IP2$ and $IP3$, respectively) are of most interest to microwave design engineers and will be discussed here, although higher levels of intercept point may be readily computed. General expressions for load-referenced $IP2$ and $IP3$ can be written for the series reflective HEMT-based switch in terms of the expansion parameters in (1) [12]. The series reflective switch has been chosen for this discussion since previous studies have shown that in single-pole double-throw (SPDT) switch topologies, the series on-state element is the primary distortion generating mechanism [12], [13]. With this in mind, the intercept points for a series-connected configuration can be written using the $I_{\rm DS}$–$V_{\rm DS}$ expansion parameters α_n as [12]

$$IP2 = \frac{Z_0 \alpha_1^4}{2\alpha_2^2}(1 + 2\alpha_1 Z_0)^2$$
$$IP3 = \frac{Z_0 \alpha_1^3}{2\alpha_3}(1 + 2\alpha_1 Z_0). \tag{2}$$

The first-order expansion parameter α_1 is the inverse of the channel series resistance R_C. Similar intercept point relationships can be derived for more complex switch circuit topologies. The equivalent circuit for the HEMT operating in a control mode is shown in Fig. 1. The gate bias resistor R_G is used to ensure that the gate is ac isolated from ground and the RF path at all frequencies because of the capacitive coupling between the gate–drain and gate–source. The resistance R_{GG} represents the gate leakage component. This leakage path is modeled in SPICE as a capacitor-diode parallel circuit; a leakage resistance replaces the reverse bias diode in this representation to simplify the analysis.

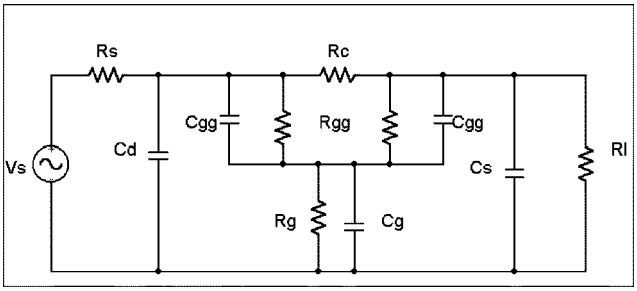

Fig. 1. AC equivalent-circuit representation for the HEMT-based microwave and RF switch, showing the gate leakage and gate bias equivalent impedances.

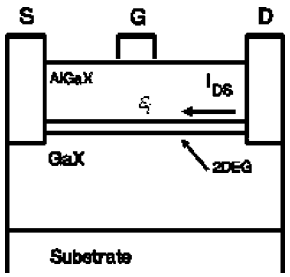

Fig. 2. Idealized structure of the a HEMT based on an AlGaX/GaX heterostructure (*X* denotes either arsenic or nitrogen). The AlGaX layer is d_i thick and the 2DEG is Δd thick.

B. HEMT I–V Characteristics

The fabrication of these high-frequency and high-speed systems is achieved by creating a heterostructure between materials with different energy bandgaps, typically the AlGaAs/GaAs system or, more recently, the AlGaN/GaN system, which creates an interface 2DEG at the metallurgical junction (Fig. 2). The electrons in this 2DEG are of very high mobility, and when coupled with the high 2DEG carrier density, a very thin, but highly conductive, layer is created. The carrier density in this layer can be modulated by the application of a control voltage on the device gate.

The I–V characteristics of the HEMT are strongly influenced by the field-dependent mobility in the 2DEG. High electric fields will occur in the conducting channel layer during control of high-power signals because of narrow gate lengths, with a corresponding reduction in the channel mobility with increasing voltage drop across the drain–source. A simple model for the velocity–electric-field profile is assumed, and the expression for the mobility is derived from the derivative of this profile [14]. Fig. 3 shows the model velocity–electric-field profile for the AlGaAs/GaAs heterostructure system. Typical values for the low field mobility and velocity saturation value in AlGaAs/GaAs and AlGaN/GaN systems are presented in Table I. In the 2DEG, a simple approximation for the electric field is V/L [10]; this approximation yields a mobility versus channel voltage relation of the form

$$\mu(V) = \frac{dv(E)}{dE} = \frac{\mu_{LF}}{\left[1 + \dfrac{\mu_{LF} V}{L v_{\rm sat}}\right]^2} = \sum_{n=0}^{\infty} \mu_n V^n. \tag{3}$$

The I–V characteristic for the HEMT is derived in a similar fashion as the MOSFET [16]; however, the carrier density in the

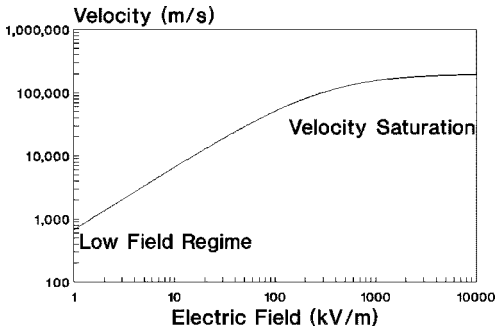

Fig. 3. Plot of the velocity–electric-field model (3) for the AlGaAs heterostructure. Values of mobility and $v_{\rm sat}$ are taken from Table I for this illustration.

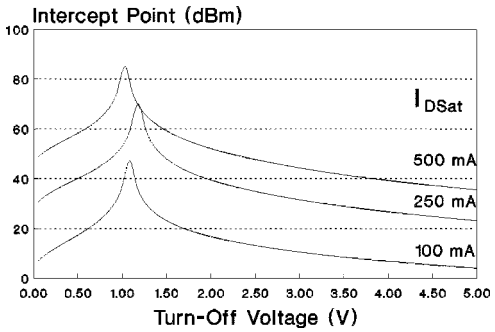

Fig. 4. Second-order distortion intercept point for the series-connected AlGaAs/GaAs HEMT microwave switch plotted versus HEMT turn-off voltage $V_{\rm Off}$ with the saturated drain current $I_{\rm DSat}$ as a parameter.

TABLE I
TABLE OF LOW FIELD MOBILITY AND SATURATION VELOCITY FOR THE 2DEG IN GaAs [15] AND GaN [11] HETEROSTRUCTURE SYSTEMS

System	AlGaAs/GaAs [15]	AlGaN/GaN [11]
μ_{LF} (m^2/V-sec)	0.68	0.06
v_{SAT} (m/sec)	2×10^5	2.5×10^5

2DEG above threshold is a function of the capacitance per unit area of the gate–2DEG structure and the gate–source voltage [16]

$$n_{\rm 2DEG} = \frac{\varepsilon_i}{q(d_i + \Delta d)} \left(V_{\rm GS} - V_{\rm Off}\right). \tag{4}$$

By assuming a linear variation of voltage in the channel (similar to MOS square law theory [16]) and the mobility relation in (3), the nonlinear drain–source current can be written as

$$I_{\rm DS} = \frac{W}{L} \frac{\varepsilon_i}{d_i + \Delta d} \mu_{LF} \sum_{n=0}^{\infty} \frac{\mu_n}{\mu_0} \cdot V_{\rm DS}^{n+1} \left[\frac{V_{\rm GS} - V_{\rm Off}}{n+1} - \frac{V_{\rm DS}}{n+2}\right] \tag{5}$$

where $\mu_{LF} = \mu_0$. Assuming low field conditions ($n = 0$ term only), the drain current can be shown to saturate at current $I_{\rm DSat}$, which occurs at an approximate value of $V_{\rm DS}$ of $(V_{\rm GS0} - V_{\rm Off})$. The gate–source voltage in (4) and (5) is composed of two terms: a dc control component $(V_{\rm GS0})$ and an ac component $(v_{\rm gs})$ caused by gate leakage, as seen in the ac equivalent circuit (Fig. 1).

The gate bias and leakage circuits cause the gate voltage $V_{\rm GS}$ to be frequency dependent and, hence, the ac operating point of the HEMT to vary with frequency as well. The effects of the gate bias circuitry manifest themselves through the gate *RC* time constant, which is composed of a gate bias resistor R_G, the gate leakage resistance R_{GG}, and the two gate capacitors $C_{\rm GS}$ or $C_{\rm GD}$. At low frequencies, the gate impedances are very high, causing the gate to effectively float. At high frequencies, however, the gate–source voltage follows the drain–source voltage due to coupling through $C_{\rm GS}$ or $C_{\rm GD}$, with the gate being referenced above ground through the gate bias resistance R_G. The relationship between $v_{\rm GS}$ and $v_{\rm DS}$ can be written from the ac equivalent-circuit representation of Fig. 1 as

$$\gamma = -\frac{v_{\rm GS}}{v_{\rm DS}} = \frac{\dfrac{Z_S Z_1}{R_C} - Z_G}{Z_1 + Z_S + 2Z_G} \tag{6}$$

where $Z_S = 1/j\omega C_S$, and Z_1 is the parallel combination of R_{GG} and $C_{\rm GS}$ or $C_{\rm GD}$. The capacitances C_S and C_D are assumed equal in this result.

From (5) and (6), the ac component of the drain–source current relationship can be written strictly as a function of the ac drain–source voltage and the devices operating characteristics

$$i_{\rm DS} = \frac{2I_{\rm DSat}}{V_{\rm Off}^2} \sum_{n=0}^{\infty} \frac{\mu_n}{\mu_{LF}} \cdot v_{\rm DS}^{n+1} \left[\frac{V_{\rm GS0} - V_{\rm Off} - \gamma v_{\rm DS}}{n+1} - \frac{v_{\rm DS}}{n+2}\right] \tag{7}$$

where $I_{\rm DSat}$ is the drain–source current $i_{\rm DS}$ at saturation for $V_{\rm GS0}$ equals zero. Equation (7) provides the means for deriving the expansion coefficients α_n, yielding the distortion parameters of the HEMT. Of interest to microwave and RF design engineers are the second- and third-order distortion components, which can be found for the HEMT from the first three expansion coefficients of (7). Expanding (7) in powers of $v_{\rm DS}$ and grouping terms, the first three expansion coefficients may be written as

$$\begin{aligned} \alpha_1 &= \frac{2I_{\rm DSat}}{V_{\rm Off}} \\ &= \frac{1}{R_C} \\ \alpha_2 &= \frac{2I_{\rm DSat}}{V_{\rm Off}} \left(0.5 \frac{\mu_1}{\mu_{LF}} - \frac{0.5 + \gamma}{V_{\rm Off}}\right) \\ \alpha_3 &= \frac{2I_{\rm DSat}}{V_{\rm Off}} \left(\frac{1}{3} \frac{\mu_2}{\mu_{LF}} - \frac{\mu_1}{\mu_{LF}} \frac{0.5\gamma + (1/3)}{V_{\rm Off}}\right) \end{aligned} \tag{8}$$

where $\mu_n (n = 1, 2)$ is the mobility expansion coefficient from (3).

The combination of (2) and (8) provides a means to compute the second- and third-order distortion intercept points for the HEMT switch. Using these equations, Figs. 4 and 5 were produced, showing $IP2$ and $IP3$ for an AlGaAs/GaAs HEMT series-connected switch as a function of the turn-off voltage $V_{\rm Off}$

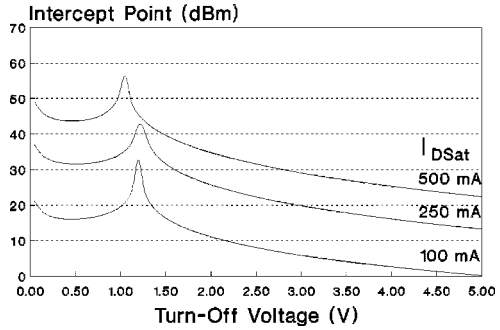

Fig. 5. Third-order distortion intercept point for the series-connected AlGaAs/GaAs HEMT microwave switch plotted versus HEMT turn-off voltage $V_{\rm Off}$ with the saturated drain current $I_{\rm Sat}$ as a parameter.

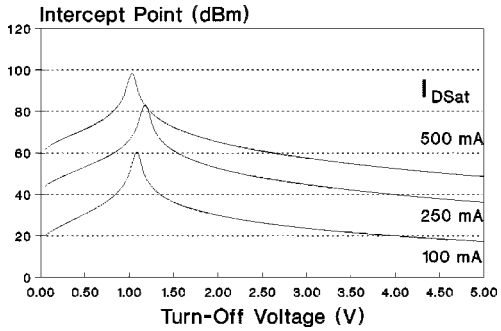

Fig. 6. Second-order distortion intercept point for the series-connected AlGaN/GaN HEMT microwave switch plotted versus turn-off voltage $V_{\rm Off}$ with the saturated drain current $I_{\rm DSat}$ as a parameter.

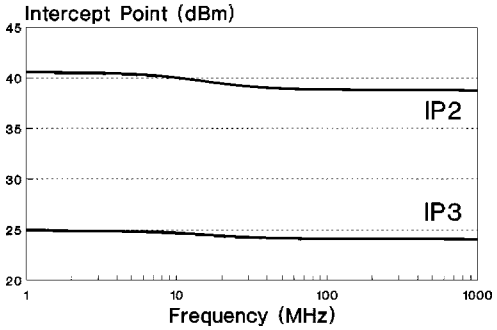

Fig. 7. Second- and third-order distortion intercept point for HEMT as a function of frequency. The devices parameters for this simulation are given in the text.

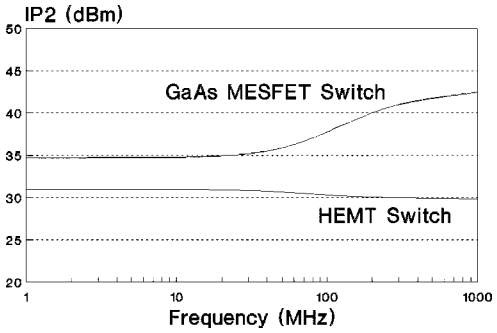

Fig. 8. Comparison of the second-order distortion intercept point $IP2$ for the HEMT and GaAs MESFET series-connected switch in the on state.

at 1000 MHz and a zero gate voltage. The drain saturation current $I_{\rm DSat}$ is used as a parameter for this illustration. The results indicate that HEMT turn-off voltages in the range of 1.0–1.5 V provide the highest levels of the distortion intercept point (implying the lowest distortion) for a given drain current saturation parameter. The peak in the intercept point is caused by phase cancellation between the nonlinearity in the 2DEG mobility and the gate bias circuitry's dependence on $V_{\rm Off}$. The figures also show improvements in distortion intercept point at any turn-off voltage with increasing $I_{\rm DSat}$, which is due to the improved insertion loss (lower channel resistance) in these devices. From (2) and (8), the level of distortion in HEMT switches can be reduced by decreasing the series R_C [increasing α_1; see (2)] of the HEMT. $I_{\rm DSat}$ and R_C may be improved by increasing the gatewidth W or decreasing the gate length L. Smaller gate lengths improve the frequency response, but increasing W will increase device capacitance and, hence, degrade the frequency response. A small positive gate voltage $(V_{\rm GS0})$ may also be used to improve R_C or $I_{\rm dsat}$. As a comparison, $IP2$ for the AlGaN/GaN HEMT switch is shown in Fig. 6. Note this similar peak in intercept point in the 1.0–1.5-V range. The overall intercept point in the AlGaN/GaN technology is higher than its AlGaAs/GaAs counterpart due to the higher saturation velocity in this device.

The HEMT exhibits a slight frequency dependence in its distortion intercept point. Fig. 7 shows the results of $IP2$ and $IP3$ simulations for an 0.25-μm gate AlGaAs HEMT with a saturated drain current of 250 mA, a turn-off voltage of −2.0 V, values of $C_{\rm GS}$ and $C_{\rm GD}$ of 0.5 pF, and a gate bias resistance of 5 KΩ. The results indicate that the distortion intercept point is higher at low frequencies (less distortion) and changes to a somewhat lower value near the gate bias circuit cutoff frequency, approximately $1/2\pi R_G(C_{\rm DG}+C_{\rm GS})$. This frequency dependence is opposite to that of GaAs MESFET switch distortion, where lower intercept points occur at low frequencies [12], [13]. This phenomenon can be explained in the following way. In the HEMT, the gate–drain and gate–source circuit couples ac voltage to the gate, causing the 2DEG sheet density (4) to vary with the applied ac signal. This effect is in contrast to bulk channel switches, such as GaAs, where the Schottky depletion layer varies with the ac signal and the channel carrier density remains constant. At low frequencies, the 2DEG sheet carrier density is somewhat higher than at high frequencies with a corresponding slight decrease in nonlinearity, giving rise to the decrease in intercept point with increasing frequency.

Fig. 8 illustrates a comparison of a second-order distortion intercept point for both an AlGaAs HEMT and GaAs MESFET series reflective switch showing the difference in frequency response between the two switch types. The parameters for each device were selected to provide identical insertion loss and with $V_{\rm Off}$ identical to the channel pinchoff voltage for the MESFET. Also note that the distortion intercept point for the GaAs MESFET switch is somewhat higher than its AlGaAs counterpart, with the difference becoming substantial (greater than 10 dB) at frequencies above their respective gate bias circuit cutoff frequencies. The third-order intercept point comparison shows similar characteristics.

The preceding discussion has focused on use of the HEMT in a series reflective switch configuration. In multithrow

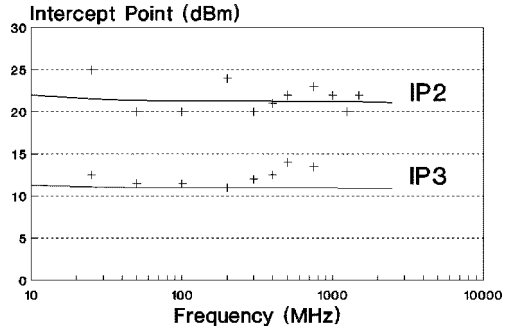

Fig. 9. Comparison of second- and third-order distortion intercept point model and measurement. The model data is denoted by a solid line and the data points are denoted by plus (+) signs.

microwave switches (such as the common four-element SPDT switch), an on-state shunt HEMT is often employed for additional protection across the receiver terminals. In these cases, an off-state series HEMT provides the primary circuit isolation, reducing the ac voltage drop across the shunt device. With this reduced voltage, the nonlinearities associated with the on-state shunt HEMT are small. However, for a single-shunt element switch, i.e., SPST, the voltage across the shunt device is higher than its series counterpart, and it is expected that the shunt configuration will generate higher levels of distortion.

III. Experimental

Second- and third-order distortion intercept point measurements were performed on a commercial AlGaAs/GaAs HEMT used as a series microwave control element. The 0.25-μm pseudomorphic HEMT used in the measurement exhibited a turn-off voltage of −1.3 V and a drain saturation current of approximately 55 mA with a gate voltage of +1.0 V. The gate control voltage was applied through a 5-kΩ resistor. A series of preliminary measurements indicated a 1-dB compression point of +11 dBm and, thus, all input powers were kept well below this level at −10 dBm. The gate capacitances were estimated from the frequency response of the insertion loss. The gate bias voltage was set for the minimum insertion loss that occurred for a gate voltage of +1.0 V. Measurements of $IP2$ and $IP3$ were performed from frequencies of 25 MHz up through 1.25 GHz, the text fixture limits. Fig. 9 shows the results of these measurements. For both $IP2$ and $IP3$, the low-frequency intercept point is higher than at high frequencies, consistent with the model. Also plotted in Fig. 9 is the model simulations for the same device. The measured data for both $IP2$ and $IP3$ are in good agreement with the model simulations, indicating the validity of the model presented.

IV. Conclusions

The origin of the distortion-generating mechanism in microwave and RF control circuits using HEMT has been discussed, and a model has been presented that can be used to predict the distortion in series-connected HEMT switches. The field-dependent mobility has been shown to be the dominant mechanism in generating distortion in these devices. The model uses such switch parameters as the channel resistance and turn-off voltage for this prediction. The model indicates that turn-off voltages in the range of 1.0–1.5 V provide the lowest distortion in series switch configurations using HEMT devices. The intercept point can be increased by decreasing the channel resistance of the HEMT. This may be accomplished by designing HEMT switch devices with smaller resistances (which will also yield lower switch insertion loss) or by applying a positive gate bias voltage in as-fabricated devices. A comparison of the HEMT switch with MESFET switches shows that the HEMT switch generates more distortion than its MESFET counterpart. In addition, the frequency response of HEMT switches is the opposite of the MESFET switch, with less distortion at low frequencies. The model is validated with experimental data taken on a GaAs HEMT in the series switch configuration

Acknowledgment

The HEMT device was supplied courtesy of Alpha Industries, Woburn, MA, with the assistance of G. Hiller. The author also wishes to thank G. Hiller for discussions on the general problem of distortion on microwave and RF control devices.

References

[1] S. Kawashi, S. Hideshisa, and K. Matsuzatani, "A novel FET model including illumination intensity parameter for simulation of optically controlled millimeter-wave oscillators," *IEEE Trans. Microwave Theory Tech.*, vol. 46, pp. 820–828, June 1998.

[2] P. Greiling and N. Ho, "Commercial satellite applications for heterojunction microelectronics technology," *IEEE Trans. Microwave Theory Tech.*, vol. 46, pp. 734–738, June 1998.

[3] C. Yuen, M. Riaziat, and S. Bandy, "Application of HEMT devices to MMICs," *Microwave J.*, vol. 31, pp. 87–88, 1988.

[4] D. L. Ingram, K. Cha, K. Hubbard, and R. Lai, "Q-band high isolation GaAs HEMT switches," in *Proc. 18th Annu. IEEE GaAs IC Symp.*, 1996, pp. 289–292.

[5] K. W. Kobayashi, A. K. Oki, L. B. Sjogren, D. K. Umemoto, T. R. Block, and D. C. Streit, "A monolithic HEMT passive switch with integrated HBT standard logic compatible driver for phased-array applications," *IEEE Microwave Guided Wave Lett.*, vol. 6, p. 375, Oct. 1996.

[6] H. Takasu, F. Sasaki, H. Kawasaki, H. Tokuda, and S. Kamihashi, "W-band SPST transistor switches," *IEEE Microwave Guided Wave Lett.*, vol. 6, pp. 315–316, Sept. 1996.

[7] Y.-F. Wu, B. P. Keller, S. Keller, D. Kapolnek, P. Kozodoy, S. P. Denbaars, and U. K. Mishra, "High power AlGaN/GaN HEMT's for microwave applications," in *Proc. Topical Workshop Heterostructure of Microelectron.*, vol. 41, 1997, pp. 1569–1574.

[8] R. Singh and C. M. Snowden, "Quasi-two-dimensional HEMT model for DC and microwave simulation," *IEEE Trans. Electron Devices*, vol. 45, pp. 1165–1169, June 1998.

[9] D. Schreurs, S. Beheydt, J. Vanhaecke, Y. Baeyens, B. Nauwelaers, W. De Raedt, M. Van Hove, and M. Van Rossum, "Characterization and modeling of HEMT's as microwave and millimeter wave MMIC switches," in *Proc. 25th European Solid-State Device Res. Conf.*, 1995, pp. 707–711.

[10] R. Singh and C. Snowden, "Small-signal characterization of microwave and millimeter-wave HEMTs," *IEEE Trans. Microwave Theory Tech.*, vol. 44, pp. 114–121, Jan. 1996.

[11] U. Mishra, Y. Wu, B. Keller, S. Keller, and D. Benbaars, "GaN microwave electronics," *IEEE Trans. Microwave Theory Tech.*, vol. 46, pp. 756–761, June 1998.

[12] R. Caverly, "Distortion in GaAs MESFET switches," *Microwave J.*, pp. 106–114, Sept. 1994.

[13] ——, "Distortion in broad-band gallium arsenide MESFET control and switch circuits," *IEEE Trans. Microwave Theory Tech.*, vol. 39, pp. 713–717, Apr. 1991.

[14] S. M. Sze, *Physics of Semiconductor Devices*, 2nd ed, New York: Wiley, 1981, pp. 324–325.

[15] K. Lee, M. Shur, T. Drummond, and H. Morkoc, "Current–voltage and capacitance-voltage characteristics of modulation-doped field effect transistors," *IEEE Trans. Electron Devices*, vol. ED-30, pp. 207–212, Mar. 1983.

[16] M. Shur and T. Fjeldly, "Compound-semiconductor field-effect transistors," in *Modern Semiconductor Device Physics*, S. M. Sze, Ed, New York: Wiley , 1998, pp. 81–135.

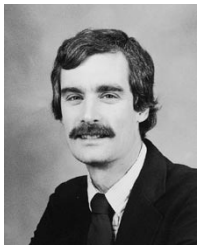

Robert H. Caverly (S'80–M'82–SM'91) was born in Cincinnati, OH, in 1954. He received the M.S.E.E. and B.S.E.E. degrees from the North Carolina State University, Raleigh, in 1978 and 1976, respectively, and the Ph.D. degree in electrical engineering from The Johns Hopkins University, Baltimore, MD, in 1983.

Since 1997, he has been a faculty member of the Department of Electrical and Computer Engineering, Villanova University, Villanova, PA. He had been with the University of Massachusetts Dartmouth (formerly Southeastern Massachusetts University), where he was a Professor. He has been a consultant for M/A-COM Inc., Burlington, MA, and Alpha Industries Inc., Woburn, MA, where he was involved in various microwave control element projects. In 1990, with support from The National Science Foundation, he was a Visiting Research Fellow with the Microwave Solid-State Group, The University of Leeds, Leeds, U.K. His research interests are characterizing p-i-n diodes and FET's in the microwave and RF control environment. His other interests include analog and digital CMOS VLSI design, an area where he has taught a number of workshops both in this country and abroad. He has published over 40 journal and conference papers in these areas.

Dr. Caverly is an Editorial Board member for the IEEE TRANSACTIONS ON MICROWAVE THEORY AND TECHNIQUES. He was a recipient of the Dow Outstanding Young Faculty Award presented by the American Society of Engineering Education.

Kennith J. Heissler received the B.S.E.E. degree from Villanova University, Villanova, PA, in 1999.

He is currently with the Engineering Leadership Development Program, Lockheed Martin Government Electronics Systems, Moorestown, NJ.